

Potential Theoretic Methods for Far Field Sound Radiation Calculations

S.I. Hariharan
Institute for Computational Mechanics in Propulsion
Lewis Research Center
Cleveland, Ohio

and The University of Akron
Akron, Ohio

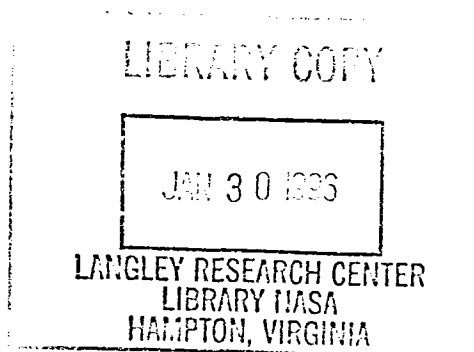
Edward J. Stenger
The University of Akron
Akron, Ohio

J.R. Scott
Lewis Research Center
Cleveland, Ohio

December 1995



National Aeronautics and
Space Administration





Potential Theoretic Methods for Far Field Sound Radiation Calculations

S. I. Hariharan

ICOMP, NASA, Lewis Research Center
Department of Mathematical Sciences
The University of Akron
Akron, OH 44325-4002

Edward J. Stenger

Department of Mathematical Sciences
The University of Akron

J. R. Scott

NASA, Lewis Research Center
Cleveland, OH 44135-3191

Mathematics Subject Classifications: 65N, 35L05, 45E, 76N

Keywords: compressible flows - aeroacoustics - singular integral equations -
far-field calculations

Proposed Running Head:
Sound Radiation Calculations

Corresponding Author:
S. I. Hariharan
ICOMP, NASA, Lewis Research Center
Department of Mathematical Sciences
The University of Akron
Akron, OH 44325-4002

email: hari@math.uakron.edu
phone: (216) 972-6994
fax: (216) 374-8630

ABSTRACT

In the area of computational acoustics, procedures which accurately predict the far-field sound radiation are much sought after. A systematic development of such procedures are found in a sequence of papers by Atassi, et. al. [3] [4] [7]. The method presented here is an alternate approach to predicting far field sound based on simple layer potential theoretic methods. The main advantages of this method are: it requires only a simple free space Green's function, it can accomodate arbitrary shapes of Kirchoff surfaces, and is readily extendable to three-dimensional problems. Moreover, the procedure presented here, though tested for unsteady lifting airfoil problems, can easily be adapted to other areas of interest, such as jet noise radiation problems. Results are presented for lifting airfoil problems and comparisons are made with the results reported in [3] [4] [7]. Direct comparisons are also made for the flat plate case.

1 INTRODUCTION

The prediction of far-field sound radiation is a key area of interest in the computational aeroacoustics community. This subject is a common intersection for most unsteady external aerodynamic problems such as the gust response of airfoils, flutter problems, and jet noise. Since these problems are posed in open domains, in general, it is difficult to extend the computational domains to the far-field due to the prohibitive cost of the computations involved. While the state of the art of computers provide high speed and large storage capacity, the numerical algorithms themselves are known to have problems. They are subject to their dissipative and dispersive properties and may contaminate acoustic calculations due to the disparity in magnitude between the acoustic pressure and the dominant flow quantities. Current efforts involving the direct numerical simulation of far-field sound are being made by Tam et. al. [11], Roe et. al. [8], and Mitchell et. al. [6]. Among all the numerical development are a sequence of works developed by Atassi and his associates [3] [4] [7]. A summary of these efforts are found in [1]. These methods employ numerical simulations in the near field, developed by Scott [9] [10], and construction of a Kirchhoff surface for the prediction of far-field sound using Green's function techniques. Thus the driving philosophy is accurate numerical simulation in the near-field and a "semi-analytical" approach to predict the far-field sound. This paper is motivated by these works. The key difference here is in the formulation of the far-field sound radiation calculations. In contrast to the work of Atassi et. al. [3] [4] [7], a potential theoretic approach is implemented. This method requires only the free space Green's function and involves an unknown simple layer density. This simple layer density is solved for by a technique proposed by Hariharan and MacCamy [5] for electromagnetic scattering problems. The application of this method for aerodynamic problems is shown here in detail. The method has the key advantage that the Kirchhoff surface does not have to be a circle or other simple shape. As long as it is a smooth surface, the method will work. This

is attractive to those studying jet noise problems, where the computational domains are typically elongated. Also, the method is extendable to fully three-dimensional problems with little difficulty.

The calculations presented here are mainly driven by the comparison of the results to those of Atassi [3] and Patrick [7] in an elliptical domain. We also compare results in a rectangular domain for a specific flat plate case presented at the ICASE/LARC Workshop on Computational Aeroacoustics [2]. The near-field calculations are performed by the GUST3D code developed by Scott [9] [10].

2 FORMULATION OF THE PROBLEM

The problem discussed here deals with the calculation of acoustic pressure in the exterior flow field Ω of some boundary Γ , where Γ is a Kirchoff surface which surrounds an arbitrary airfoil. The airfoil is submersed in a subsonic compressible flow field with a three-dimensional upstream vortical disturbance. The disturbance has magnitude and frequency vectors given by \mathbf{a} and \mathbf{k} respectively and the details of this disturbance are outlined in reference [9]. We assume that the acoustic pressure on Γ is known. The governing continuity and momentum equations for compressible subsonic flow are as follows:

$$\rho_t + \text{div}(\rho \mathbf{U}) = 0 \quad (1)$$

$$\mathbf{U}_t + (\mathbf{U} \cdot \nabla) \mathbf{U} + \frac{1}{\rho} \nabla p = 0 \quad (2)$$

and the state equations relating p and ρ are

$$p = A\rho^\gamma, \quad \frac{\partial p}{\partial \rho} = c_0^2 \quad (\gamma = 1.4 \text{ for standard air}) \quad (3)$$

where ρ is density, p is pressure, \mathbf{U} is the fluid velocity, t is time, A is a constant, and c_0 is the speed of sound. We assume that Γ is far enough from

the airfoil so that the mean flow quantities do not differ appreciably from the free stream in Ω and linearize (1) and (2) above using

$$\begin{aligned}\mathbf{U} &= \mathbf{U}_\infty + \mathbf{u} \\ \rho &= \rho_\infty + \rho' \\ p &= p_\infty + p'.\end{aligned}\tag{4}$$

\mathbf{U}_∞ , ρ_∞ , and p_∞ are the freestream velocity, density, and pressure respectively, and similarly, \mathbf{u} , ρ' and p' are the perturbation velocity, density and pressure. Before proceeding, we note that the following relation may be derived using (3) and the linearization in (4):

$$p' = c_\infty^2 \rho'.\tag{5}$$

Substituting (4) into (1) and (2), one obtains the linearized continuity and momentum equations:

$$\frac{D_0}{Dt} \rho' + \rho_\infty \operatorname{div} \mathbf{u} = 0\tag{6}$$

$$\rho_\infty \frac{D_0}{Dt} \mathbf{u} + \nabla p' = 0\tag{7}$$

where $\frac{D_0}{Dt} = \frac{\partial}{\partial t} + U_\infty \frac{\partial}{\partial x_1}$. Now, we substitute (5) into (6) and (7) to obtain

$$\frac{1}{c_\infty^2} \frac{D_0}{Dt} p' + \rho_\infty \operatorname{div} \mathbf{u} = 0\tag{8}$$

$$\rho_\infty \frac{D_0}{Dt} \mathbf{u} + \nabla p' = 0.\tag{9}$$

Manipulating (8) and (9), namely $\frac{D_0}{Dt}(8) - \operatorname{div}(9)$, yields

$$\frac{1}{c_\infty^2} \frac{D_0^2}{Dt^2} p' - \nabla^2 p' = 0$$

or

$$\frac{1}{c_\infty^2} \left(\frac{\partial}{\partial t} + U_\infty \frac{\partial}{\partial x_1} \right)^2 p' = \Delta p'.\tag{10}$$

Now, we non-dimensionalize (10) as follows:

$$\begin{aligned} x_1, x_2, x_3 & \text{ by } c/2 \\ t & \text{ by } c/2U_\infty \\ k_1, k_2, k_3 & \text{ by } 2/c \\ p' & \text{ by } \rho_\infty U_\infty |a| \end{aligned}$$

where c is the airfoil chord length. Then the dimensionless form of (10) is

$$M_\infty^2 \left(\frac{\partial}{\partial t} + \frac{\partial}{\partial x_1} \right)^2 p' = \nabla^2 p'. \quad (11)$$

We then make the following transformation which removes the dependence on time t , and the spanwise coordinate x_3 :

$$p' = \bar{p}(x_1, x_2) e^{-ik_1 t + ik_3 x_3} e^{-iK_1 x_1}.$$

The nondimensional wave number k_1 is called the reduced frequency and is given by $k_1 = \omega c/2U_\infty$ (the dimensional k_1 is given by $k_1 = \omega/U_\infty$, where ω is the dimensional angular frequency). The quantity K_1 is defined by

$$K_1 = \frac{k_1 M_\infty^2}{\beta_\infty^2}, \text{ where } \beta_\infty = \sqrt{1 - M_\infty^2}.$$

(11) then becomes

$$\beta_\infty^2 \frac{\partial^2 \bar{p}}{\partial x_1^2} + \frac{\partial^2 \bar{p}}{\partial x_2^2} + \left(\frac{k_1^2 M_\infty^2}{\beta_\infty^2} - k_3^2 \right) \bar{p} = 0. \quad (12)$$

Finally, we transform the coordinate system to the well-known Prandtl-Glauert plane using the linear transformation

$$\begin{aligned} \tilde{x}_1 &= x_1 \\ \tilde{x}_2 &= \beta_\infty x_2 \\ \tilde{x}_3 &= \beta_\infty x_3. \end{aligned}$$

Since the quantity β_∞ is less than unity, this amounts to a compression of the x_2 and x_3 coordinates. After applying this transformation, we have

$$\tilde{\nabla}^2 \bar{p} + K^2 \bar{p} = 0, \quad (13)$$

where

$$K^2 = \frac{k_1^2 M_\infty^2}{\beta_\infty^4} - \frac{k_3^2}{\beta_\infty^2}.$$

Now the problem clearly becomes a classical exterior problem governed by the Helmholtz equation (13) subject to numerically calculated values of \bar{p} on the boundary $\tilde{\Gamma}$, where $\tilde{\Gamma}$ is the transformed boundary in the Prandtl-Glauert plane. Even though it appears to be a simple problem, the assembly of solutions plays a major role in the accurate prediction of far field calculations. A procedure that has a general structure is proposed here and is described next.

3 SOLUTION PROCEDURE

The solution procedure is based on simple layer potential theory [5]. The advantage of the procedure is that the solution relies on a free space Green's function rather than a specific Green's function which is suited for the domain of the problem. In particular, arbitrarily shaped Kirchhoff surfaces may be used. The free space Green's function for (13) is

$$G(\tilde{\mathbf{x}}, \tilde{\mathbf{y}}) = -\frac{i}{4} H_0^1(K |\tilde{\mathbf{x}} - \tilde{\mathbf{y}}|), \quad (14)$$

where $\tilde{\mathbf{x}}$ is a point in the transformed domain, $\tilde{\Omega}$, and $\tilde{\mathbf{y}}$ is a point on $\tilde{\Gamma}$.

From potential theory [5], the solution of (13) can be written as

$$\bar{p}(\tilde{\mathbf{x}}) = \int_{\tilde{\Gamma}} \sigma(\tilde{\mathbf{y}}) G(\tilde{\mathbf{x}}, \tilde{\mathbf{y}}) ds_{\tilde{\mathbf{y}}} \quad \tilde{\mathbf{x}} \in \tilde{\Omega}, \quad \tilde{\mathbf{y}} \in \tilde{\Gamma} \quad (15)$$

where \bar{p} satisfies

- $\bar{p} \sim \frac{e^{iKR}}{\sqrt{R}}$ as $|\tilde{\mathbf{x}}| \rightarrow \infty$ with $R = |\tilde{\mathbf{x}} - \tilde{\mathbf{y}}|$

- $\bar{p} = \tilde{f}(\tilde{\mathbf{x}})$ on $\tilde{\Gamma}$.

Imposing the boundary condition, (15) becomes

$$\int_{\tilde{\Gamma}} \sigma(\tilde{\mathbf{y}}) G(\tilde{\mathbf{x}}, \tilde{\mathbf{y}}) ds_{\tilde{\mathbf{y}}} = \tilde{f}(\tilde{\mathbf{x}}), \quad \tilde{\mathbf{x}}, \tilde{\mathbf{y}} \in \tilde{\Gamma}. \quad (16)$$

We can now describe a procedure for solving (16) for the σ values. Upon calculating σ and substituting in (15), \bar{p} at any point $\tilde{\mathbf{x}} \in \tilde{\Omega}$ can be determined.

To allow an arbitrary shape of the Kirchoff surface, it will be assumed that $\tilde{\Gamma}$ is some polar representable geometry. Therefore, it can be expressed as the function $r = R(\theta)$. Let θ and ϕ be polar representations of the points $\tilde{\mathbf{x}}$ and $\tilde{\mathbf{y}}$ respectively. Then $\tilde{\mathbf{x}}$ and $\tilde{\mathbf{y}}$ may be expressed in polar coordinates as

$$\begin{aligned} \tilde{\mathbf{x}}(\theta) &= (R(\theta) \cos \theta, R(\theta) \sin \theta) \\ \tilde{\mathbf{y}}(\phi) &= (R(\phi) \cos \phi, R(\phi) \sin \phi), \end{aligned}$$

and we may write

$$\tilde{f}(\tilde{\mathbf{x}}) = \tilde{f}(R(\theta) \cos \theta, R(\theta) \sin \theta) \equiv \hat{f}(\theta),$$

and

$$\sigma(\tilde{\mathbf{y}}) = \sigma(R(\phi) \cos \phi, R(\phi) \sin \phi) \equiv \hat{\sigma}(\phi).$$

The distance between the two points $\tilde{\mathbf{x}}$ and $\tilde{\mathbf{y}}$ is then given by

$$\begin{aligned} |\tilde{\mathbf{x}} - \tilde{\mathbf{y}}| &= |(R(\theta) \cos \theta, R(\theta) \sin \theta) - (R(\phi) \cos \phi, R(\phi) \sin \phi)| \\ &= \sqrt{R^2(\theta) + R^2(\phi) - 2R(\theta)R(\phi) \cos(\theta - \phi)} \\ &\equiv d(\theta, \phi), \end{aligned} \quad (17)$$

and the Green's function becomes

$$\begin{aligned} G(\tilde{\mathbf{x}}, \tilde{\mathbf{y}}) &= -\frac{i}{4} H_0^{(1)}(K |\tilde{\mathbf{x}} - \tilde{\mathbf{y}}|) \\ &= -\frac{i}{4} H_0^{(1)}(K d(\theta, \phi)) \\ &\equiv \hat{G}(\theta, \phi). \end{aligned} \quad (18)$$

Now, since $\tilde{y} = (\tilde{x}, \tilde{y})$, where \tilde{x} and \tilde{y} are given by

$$\begin{aligned}\tilde{x} &= R(\phi) \cos \phi \\ \tilde{y} &= R(\phi) \sin \phi,\end{aligned}$$

$d\tilde{x}$ and $d\tilde{y}$ are given by

$$\begin{aligned}d\tilde{x} &= [-R(\phi) \sin \phi + R'(\phi) \cos \phi] d\phi \\ d\tilde{y} &= [R(\phi) \cos \phi + R'(\phi) \sin \phi] d\phi\end{aligned}$$

and ds is as follows:

$$\begin{aligned}ds &= \sqrt{d\tilde{x}^2 + d\tilde{y}^2} \\ &= \sqrt{[R'(\phi) \cos \phi - R(\phi) \sin \phi]^2 + [R'(\phi) \sin \phi + R(\phi) \cos \phi]^2} d\phi \\ &= \sqrt{R'^2(\phi) + R^2(\phi)} d\phi.\end{aligned}$$

Substituting the above quantities into (15) yields

$$\hat{f}(\theta) = \int_0^{2\pi} \sigma(\phi) \hat{G}(\theta, \phi) \sqrt{R'^2(\phi) + R^2(\phi)} d\phi, \quad \theta \in [0, 2\pi).$$

By defining $\bar{\sigma}(\phi) = \sigma(\phi) \sqrt{R'^2 + R^2}$, we obtain our final equation

$$\hat{f}(\theta) = \int_0^{2\pi} \bar{\sigma}(\phi) \hat{G}(\theta, \phi) d\phi, \quad \theta \in [0, 2\pi). \quad (19)$$

We now consider the case where $\theta = \phi$ in (18) and \hat{G} becomes singular. We must first note that the zero order Hankel function of the first kind may be expressed by

$$-\frac{i}{4} H_0^{(1)}(z) = \frac{1}{2\pi} \log(z) + \hat{\gamma} - \frac{i}{4} + \hat{R}(z),$$

where $\hat{\gamma} = \frac{\gamma - \log 2}{2\pi}$ (γ is Euler's constant and $\hat{R}(z) \rightarrow 0$ as $z \rightarrow 0$). Using this, \hat{G} may be written as follows:

$$\begin{aligned}\hat{G}(\theta, \phi) &= -\frac{i}{4} H_0^{(1)}(K d(\theta, \phi)) \\ &= \frac{1}{2\pi} \log(K d(\theta, \phi)) + \hat{\gamma} - \frac{i}{4} + \hat{R}(K d(\theta, \phi)).\end{aligned} \quad (20)$$

Our next step is to observe that when $\theta \rightarrow \phi$, $R(\theta)$ can be expanded in a neighborhood of ϕ by a Taylor series in the following way:

$$R(\theta) = R(\phi) + R'(\phi)(\theta - \phi) + \frac{R''(\phi)}{2!}(\theta - \phi)^2 + \dots$$

Next, we square (17) and substitute the above for $R(\theta)$ to obtain

$$\begin{aligned} d^2(\theta, \phi) &= 4R^2(\phi) \sin^2\left(\frac{\theta - \phi}{2}\right) + 4R(\phi)R'(\phi) \sin^2\left(\frac{\theta - \phi}{2}\right)(\theta - \phi) \\ &\quad + [R'^2(\phi) + 2R(\phi)R''(\phi) \sin^2\left(\frac{\theta - \phi}{2}\right)](\theta - \phi)^2 \\ &\quad + \left[\frac{1}{2}R'(\phi)R''(\phi) + \frac{2}{3}R(\phi)R'''(\phi) \sin^2\left(\frac{\theta - \phi}{2}\right)\right](\theta - \phi)^3 + \dots \end{aligned}$$

Now we divide both sides by the first term on the right hand side and take the limit as $\theta \rightarrow \phi$ to obtain

$$\lim_{\theta \rightarrow \phi} \frac{d^2(\theta, \phi)}{4R^2(\phi) \sin^2\left(\frac{\theta - \phi}{2}\right)} = 1 + \frac{R'^2(\phi)}{R^2(\phi)}.$$

Thus, when $\theta \rightarrow \phi$,

$$d(\theta, \phi) = 2 \sin\left(\frac{|\theta - \phi|}{2}\right) \sqrt{R'^2(\phi) + R^2(\phi)}. \quad (21)$$

This confines the singularity which arises in (20) to the factor $\sin\left(\frac{|\theta - \phi|}{2}\right)$.

Our next step is to rewrite (19) as follows:

$$\int_0^{2\pi} (\bar{\sigma}(\phi) - \bar{\sigma}(\theta)) \hat{G}(\theta, \phi) d\phi + \bar{\sigma}(\theta) \int_0^{2\pi} \hat{G}(\theta, \phi) d\phi \equiv \hat{g}(\theta), \quad \theta \in [0, 2\pi). \quad (22)$$

The motivation for doing this is that when $\theta \rightarrow \phi$, it can be shown [5] that the first term in (22) will approach zero, and we may use (21) to work with the singularity in the last term of (22). Substituting (20) in the last term of (22) gives

$$\begin{aligned} &\bar{\sigma}(\theta) \int_0^{2\pi} \hat{G}(\theta, \phi) d\phi \\ &= \bar{\sigma}(\theta) \int_0^{2\pi} \left[\frac{1}{2\pi} \log(2K \sqrt{R'^2(\phi) + R^2(\phi)} \sin\left[\frac{|\theta - \phi|}{2}\right]) + \hat{\gamma} - \frac{i}{4} + \hat{R}(\theta, \phi) \right] d\phi \\ &= \bar{\sigma}(\theta) \int_0^{2\pi} \log\left[\sin\left(\frac{|\theta - \phi|}{2}\right)\right] d\phi + \bar{\sigma}(\theta) \int_0^{2\pi} \hat{R}(\theta, \phi) d\phi, \quad \theta \in [0, 2\pi) \end{aligned} \quad (23)$$

where \bar{R} is defined by

$$\bar{R} = \begin{cases} \hat{\gamma} - \frac{i}{4} + \frac{1}{2\pi} \log(2K\sqrt{R'^2(\phi) + R^2(\phi)}), & \theta = \phi \\ -\frac{i}{4}H_0^{(1)}(Kd(\theta, \phi)) - \frac{1}{2\pi} \log(\sin[\frac{|\theta-\phi|}{2}]), & \theta \neq \phi \end{cases}$$

Now, we must turn our attention to the first term in (23). Using complex analysis, the exact value of this integral may be obtained, namely

$$\int_0^{2\pi} \log[\sin(\frac{|\theta - \phi|}{2})] d\phi = -2\pi \log(2).$$

Using this result in (22) gives us the following:

$$\begin{aligned} & \int_0^{2\pi} (\bar{\sigma}(\phi) - \bar{\sigma}(\theta)) \hat{G}(\theta, \phi) d\phi \\ & - \bar{\sigma}(\theta) \log(2) + \bar{\sigma}(\theta) \int_0^{2\pi} \bar{R}(\theta, \phi) d\phi = \hat{g}(\theta), \quad \theta \in [0, 2\pi). \end{aligned} \quad (24)$$

With this equation, we have removed the problem of the singularity in (19) and are now ready to attempt to numerically find the $\bar{\sigma}$ values.

4 NUMERICAL PROCEDURE

To numerically determine the solution, we must first choose a suitable shape for the Kirchhoff surface. The choice of an ellipse, specifically a circle, will greatly simplify the above formulation since analytical representations for $R(\theta)$ and its derivative are well known. If we choose some other shape, we may have to numerically approximate $R'(\theta)$, thereby reducing accuracy. The Kirchhoff surface must also be far enough away from the airfoil so that the mean flow quantities on $\tilde{\Gamma}$ deviate only slightly from those of the free stream. We may then use the GUST3D code to determine the values of \bar{p} at a finite number of points on the boundary.

A numerical representation of (24) can be obtained using rectangular quadrature. Letting $a = 0$, $b = 2\pi$, $h_j = \phi_j - \phi_{j-1}$, and $h_i = \theta_i - \theta_{i-1}$,

equation (24) becomes

$$\begin{aligned} & \sum_{j=1}^{n-1} [\bar{\sigma}(\phi_j) - \bar{\sigma}(\theta)] \hat{G}(\theta, \phi_j) h_{j+1} \\ & - \bar{\sigma}(\theta) \log(2) + \bar{\sigma}(\theta) \sum_{j=1}^{n-1} \bar{R}(\theta, \phi_j) h_{j+1} = \hat{f}(\theta). \end{aligned}$$

Noting that both θ and ϕ correspond to points on $\tilde{\Gamma}$, we may replace θ by θ_i and obtain

$$\begin{aligned} & \sum_{j=1}^{n-1} [\bar{\sigma}(\phi_j) - \bar{\sigma}(\theta_i)] \hat{G}(\theta_i, \phi_j) h_{j+1} \\ & - \bar{\sigma}(\theta_i) \log(2) + \bar{\sigma}(\theta_i) \sum_{j=1}^{n-1} \bar{R}(\theta_i, \phi_j) h_{j+1} = \hat{f}(\theta_i) \end{aligned} \quad (25)$$

For each i from 1 to $n-1$, an equation of the above type will be yielded. We will have $n-1$ equations and $n-1$ unknowns (the $\bar{\sigma}$ values), and therefore it would be to our benefit to represent (25) as

$$\sum_{j=1}^{n-1} A_{ij} \bar{\sigma}_j = \hat{f}_i$$

where $A_{ij} = A(\theta_i, \phi_j)$, $\bar{\sigma}_j = \bar{\sigma}(\phi_j)$ and $\hat{f}_i = \hat{f}(\theta_i)$. With (25) in this form, we could use a matrix solver to solve the augmented matrix yielded by the system of equations. After some scrutinization of (25), it can be seen that the values used for A_{ij} should be as follows:

$$A_{ij} = \begin{cases} -\log(2) + [\sum_{k=1}^{n-1} \bar{R}_{ik} h_{k+1} - \sum_{k=1, (k \neq i)}^{n-1} \hat{G}_{ik} h_{k+1}], & i = j \\ \hat{G}_{ij} h_{j+1}, & i \neq j \end{cases}$$

where $\bar{R}_{ij} = \bar{R}(\theta_i, \phi_j)$ and $\hat{G}_{ij} = \hat{G}(\theta_i, \phi_j)$.

Once our goal of finding the $\bar{\sigma}$ values is reached, it is a rather simple matter to obtain \bar{p} at any point $\mathbf{x} \in \Omega$. Since our solution procedure was derived in terms of $\tilde{\Gamma}$ and $\tilde{\Omega}$, in order to find the solution at some point $\mathbf{x} \in \Omega$ we must first transform it to a point $\tilde{\mathbf{x}} \in \tilde{\Omega}$. Once we have a point $\tilde{\mathbf{x}} \in \tilde{\Omega}$, we

can use the solution procedure outlined above. For simplicity of notation, let (r, θ) and (r, ϕ) be polar representations of the points \tilde{x} and \tilde{y} respectively, and proceed as follows. Let $\tilde{x} \in \tilde{\Omega}$ be represented as

$$\tilde{x} = (r \cos \theta, r \sin \theta)$$

where r and θ are fixed, and let $\tilde{y} \in \tilde{\Gamma}$ be defined as follows:

$$\tilde{y} = (R(\phi) \cos \phi, R(\phi) \sin \phi), \quad \phi \in [0, 2\pi).$$

Therefore, the distance between \tilde{x} and \tilde{y} is given by

$$\begin{aligned} |\tilde{x} - \tilde{y}| &= \sqrt{[r \cos \phi - R(\phi) \cos \phi]^2 + [r \sin \theta - R(\phi) \sin \phi]^2} \\ &= \sqrt{r^2 + R^2(\phi) - 2rR(\phi) \cos(\theta - \phi)} \\ &= d(r, \theta, \phi), \end{aligned}$$

and the Green's function becomes

$$\hat{G}(\theta, \phi) = -\frac{i}{4} H_0^{(1)}(K d(r, \theta, \phi)).$$

As follows from (20), the solution will be

$$\bar{p}(r, \theta) = -\frac{i}{4} \int_0^{2\pi} \bar{\sigma}(\phi) H_0^{(1)}(K d(r, \theta, \phi)) d\phi.$$

This can be expressed numerically as

$$\bar{p}(r, \theta) = -\frac{i}{4} \sum_{j=1}^{n-1} \bar{\sigma}(\phi_j) H_0^{(1)}(K d(r, \theta, \phi_j)) h_{j+1}.$$

5 RESULTS AND DISCUSSION

All calculations use the above described method, where the GUST3D code is used to predict the pressure on the Kirchhoff surface. A circular boundary centered at the center of the airfoil is used and the pressure values interpolated from those provided by GUST3D using cubic spline interpolation.

The number of data points on the Kirchhoff surface is a function of reduced frequency; from 40 points for lower frequencies to 80 for higher frequencies (see references [9] and [10] for details). The system of equations generated is solved using Gaussian elimination with pivoting. The radius of the Kirchhoff Surface is 1.5 times the semichord for flat plates. For airfoils with thickness, the radius is the minimum radius for which the mean flow and freestream velocities differ by less than 5% and typically varies from 1.3-2.5 times the semichord. Increasing or decreasing this radius by a small amount does not significantly alter the solution as is indicated in figure 15.

5.1 ICASE Benchmark Problem 6

In this case we have a flat plate in a transverse gust (see figure 2.b) defined as

$$v = 0.1c_\infty \sin \left[\frac{\pi}{8} \left(\frac{x}{M_\infty} - t \right) \right]$$

where the normalization for the velocity is with respect to c_∞ ; length with respect to $\Delta x = 1$; and time, with respect to $\Delta x/c_\infty$. The Mach number is given as 0.5, and the chord length is 30 units. Using our non-dimensionalization, we get $k_1 = 15\pi/4 = 11.781$ and $a_2 = 0.2$. The unsteady pressure is to be calculated on a box surrounding the flat plate as shown in figure 1. The sides of the box are located at dimensional positions of $x_1 = \pm 95$ and $x_2 = \pm 95$. When non-dimensionalized by the semichord, the values are $x_1 = \pm 6.333$ and $x_2 = \pm 6.333$.

The rms pressure, $(\frac{1}{2}|p'|^2)$, is determined on the sides of the box and compared to those obtained by Patrick and Atassi [2] using a semi-analytical approach in figures 3-6. 100 data points per side were used. The results compare quite well, considering that the acoustic energy is such a small fraction of the total flow energy, and highly accurate results are difficult to obtain.

5.2 Polar Plot Comparisons

Polar plots of the solution on a circle of radius r were made, where a value of 100 times the semichord was used for r . This value is quite arbitrary and, in fact, the solution was multiplied by \sqrt{r} to remove the dependence on r . The solution was determined at 200 evenly spaced data points on the circle.

Direct comparisons to those of Atassi and Patrick [7] were made for the flat plate case for reduced frequency values of 1.0 and 3.0 and Mach numbers 0.1, 0.5 and 0.8 in a transverse gust (see figure 2.b). These are compared in figures 7-12 and only very slight differences are observed.

In figures 13-14, we examine the effects of airfoil thickness for symmetric airfoils at no angle of attack in a transverse gust for the Mach numbers and reduced frequencies given above. Several examples of polar plots of the far field solution for airfoils with camber and angle of attack in both transverse and oblique (see figure 2.b) gusts are shown in figures 16-20. These serve as a demonstration of what kind of information can be gleaned from this method. As the purpose of this paper is to simply present the potential theoretic approach to determine far field acoustics as an alternative to other Green's functions methods, we will not go into any indepth analysis of these plots. However, the expected results are obtained for these cases (see references [3] and [7]) with only minor discrepancies, although no direct comparisons to the results of Atassi and Patrick are available at this time.

6 CONCLUSION

It was shown that potential theoretic methods are a viable alternative to the modified Green's function approach of Atassi for obtaining the far field acoustic radiation from lifting airfoils. The only numerical techniques needed are rectangular quadrature, Gauss-Jordan elimination with pivoting, and cubic spline interpolation- all of which are simple, well-established techniques. Moreover, the method does not require the development of a new Green's

function but uses the well-known free space Green's function. This allows for easy extendability to completely three-dimensional problems, i.e., the solution is represented as a surface integral and the three-dimensional free space Green's function for the Helmholtz operator is used. Future work is planned along these lines.

REFERENCES

1. H.M. Atassi, *Unsteady Aerodynamics of Vortical Flows: Early and Recent Developments*, Symposium on Aerodynamics and Aeroacoustics, Feb. 28-March 2, 1993.
2. H.M. Atassi and S.M. Patrick, *Semianalytical Solution for the Far Field of a Gust Interacting with a Flat Plate Airfoil*, ICASE/LARC Workshop on Computational Aeroacoustics, Hampton. Oct. 24-6, 1994.
3. H.M. Atassi, S. Subramaniam and J.R. Scott, *Acoustic Radiation from Lifting Airfoils in Compressible Subsonic Flows*, AIAA Paper 90-3911, October, 1990.
4. H.M. Atassi, M. Dusey and C.M. Davis, *Acoustic Radiation from a Thin Airfoil in Nonuniform Subsonic Flows*, AIAA Paper 90-3910, October, 1990.
5. S.I. Hariharan and R.C. MacCamy, *Integral Equation Procedures for Eddy Current Problems*, J. Comput. Phys. Vol. 45, No. 1, January, 1982.
6. B.E. Mitchell, S.K. Lele and P. Moiu, *Computations of the Far-field Sound Radiated by an Axisymmetric Jet*, Flow Acoustics: A Technology Audit, Ecole Centrales de Lyon, France. July 11-13, 1994.
7. S.M. Patrick, C.M. Davis and H.M. Atassi, *Acoustic Radiation from a Lifting Airfoil in Nonuniform Subsonic Flows*, FED-Vol. 147, Computational Aero- and Hydro-Acoustics, ASME 1993.
8. P. Roe, *Linear Bicharacteristic Schemes Without Dissipation*, ICASE Report No. 94-65, July, 1994.(unpublished)

9. J.R. Scott, *Compressible Flows with Periodic Vortical Disturbances Around Lifting Airfoils*, Ph. D. Dissertation, University of Notre Dame, IN, May, 1990.(unpublished)
10. J.R. Scott and H.M. Atassi, *A Finite-Difference, Frequency-Domain Numerical Scheme for the Solution of the Gust Response Problem*, J. Comput. Phys., Vol. 119, 1995, pp. 75-93.
11. C.K.W. Tam and J.C. Webb, *Dispersion-Relation-Preserving Schemes for Computational Acoustics*, J. Comput. Phys., Vol. 107, 1993, pp. 262-281.

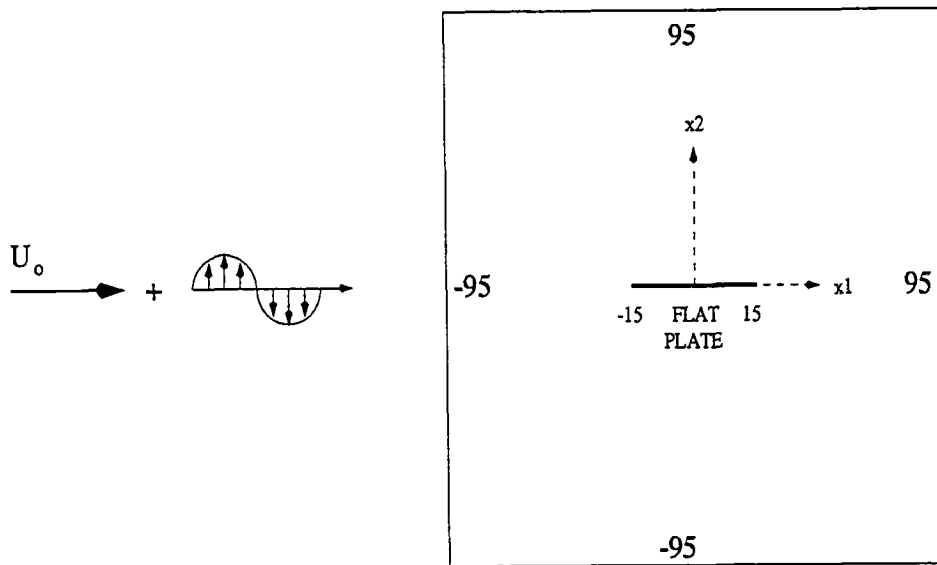
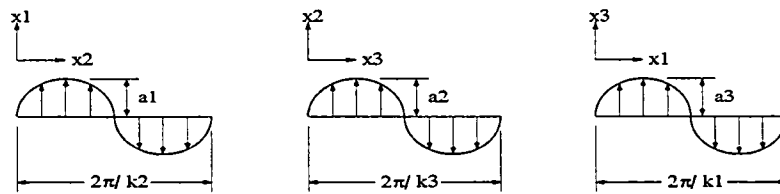


Figure 1- ICASE Benchmark Problem 6



Three-dimensional (oblique) gust configuration

$$\mathbf{a} \cdot \mathbf{k} = 0$$

$$|\mathbf{a}| = 1$$

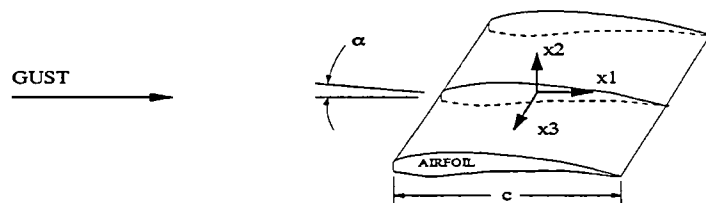


Figure 2.a

Airfoil in a Transverse Gust

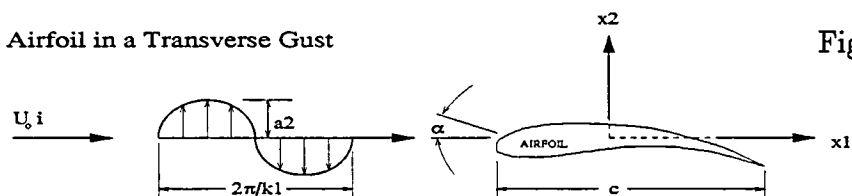


Figure 2.b

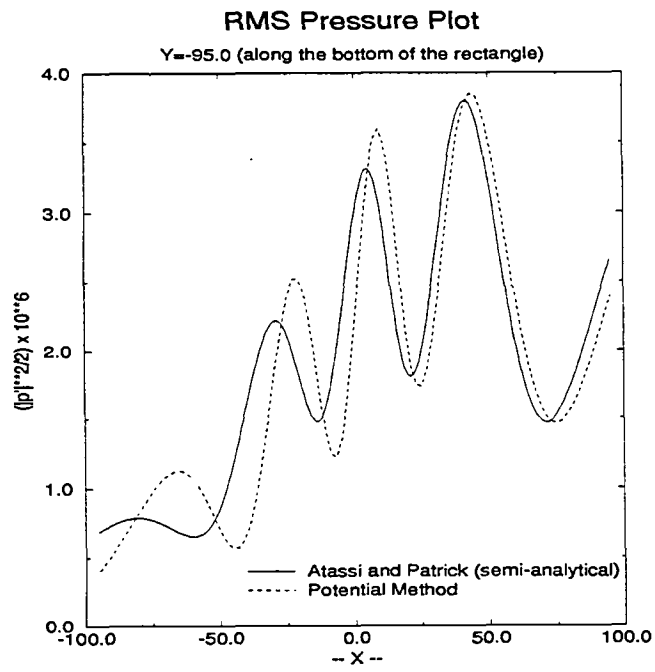


Figure 3.

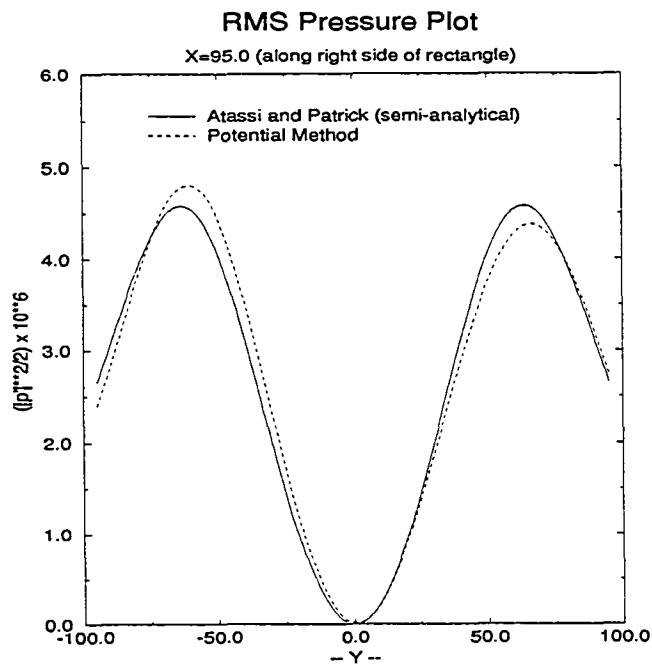


Figure 4.

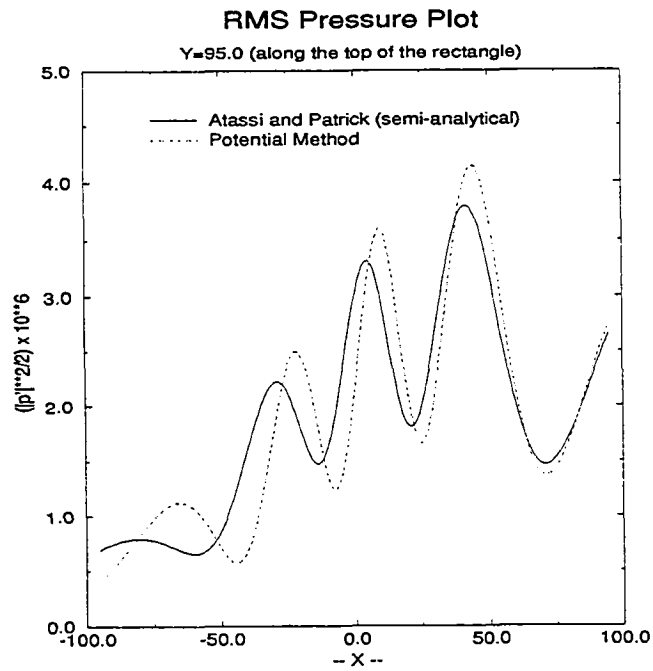


Figure 5.

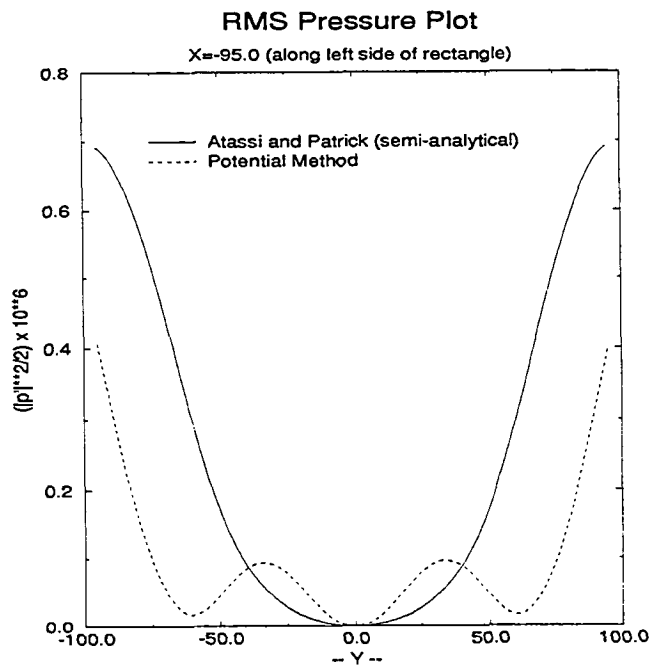


Figure 6.

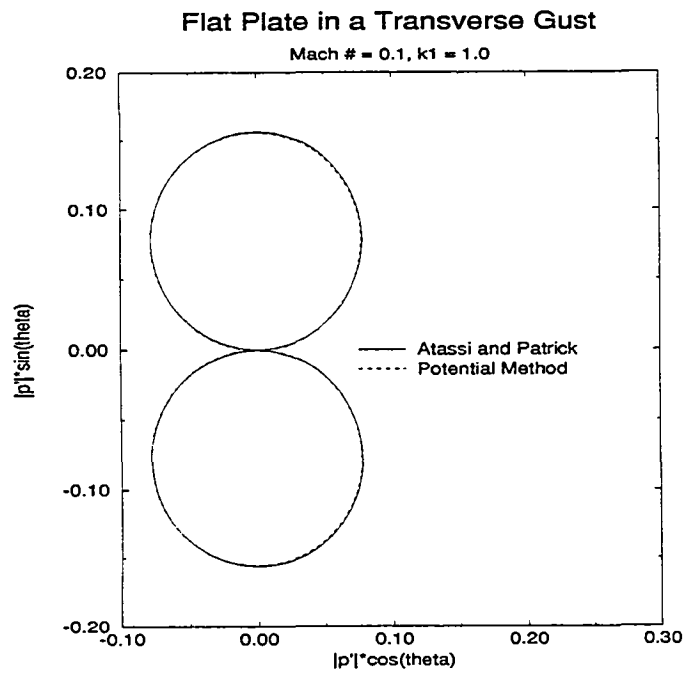


Figure 7.

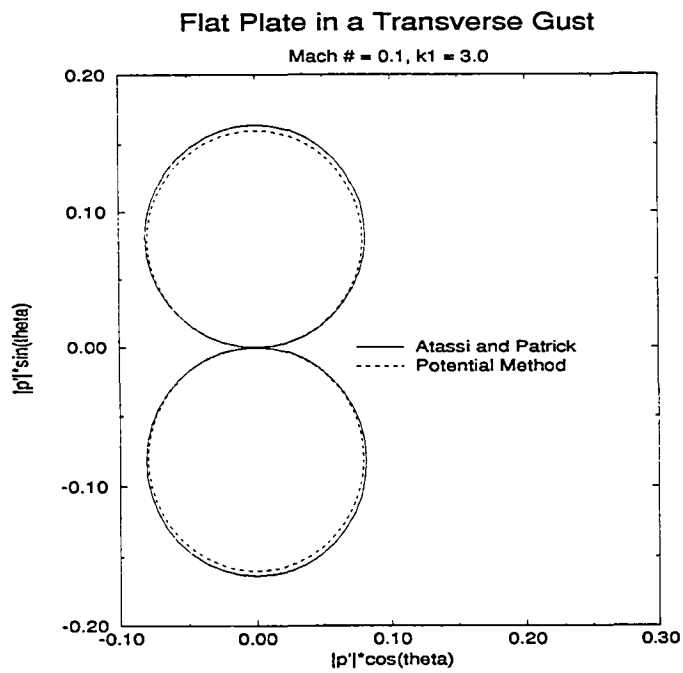


Figure 8.

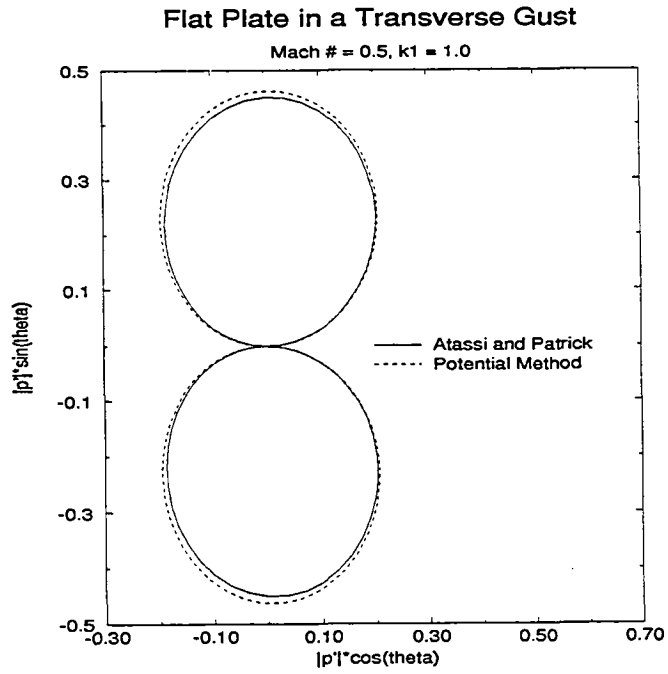


Figure 9.

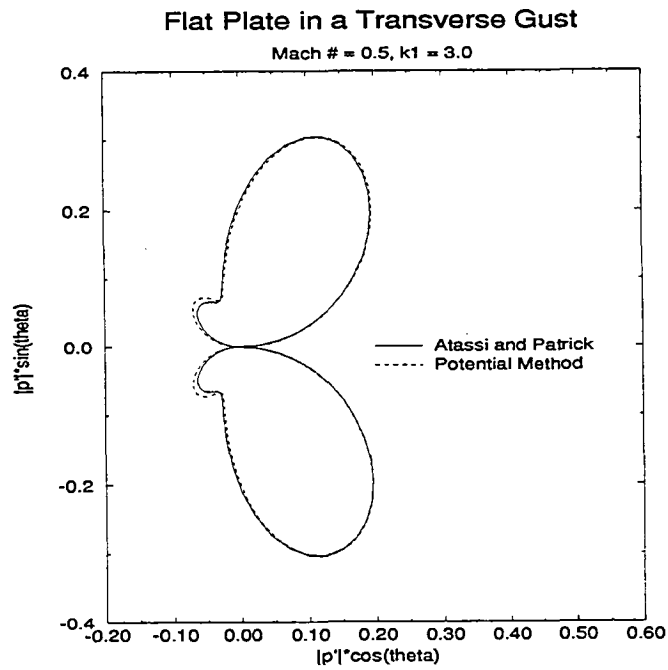


Figure 10.

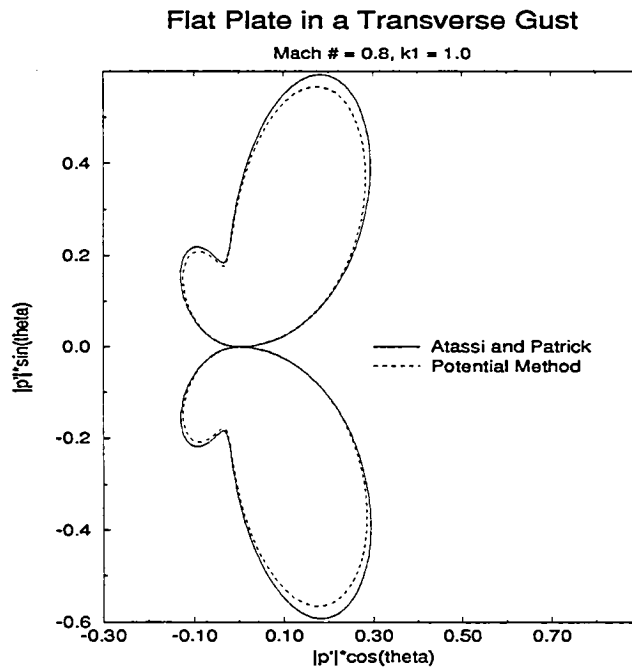


Figure 11.

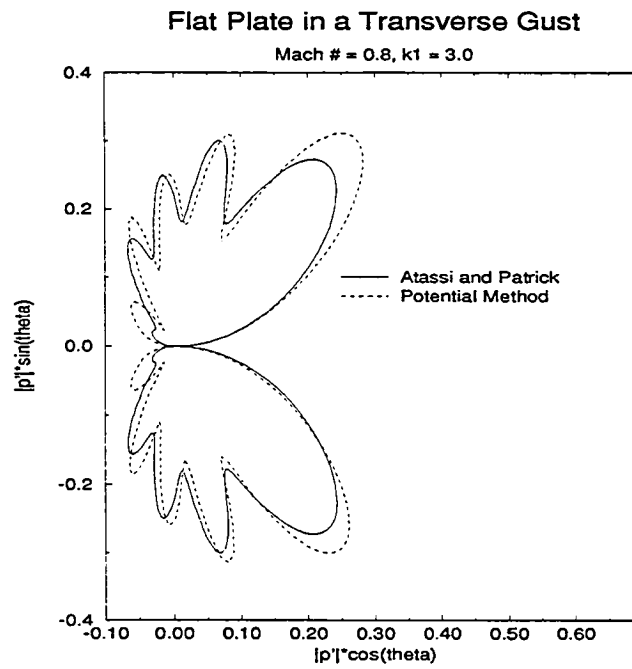


Figure 12.

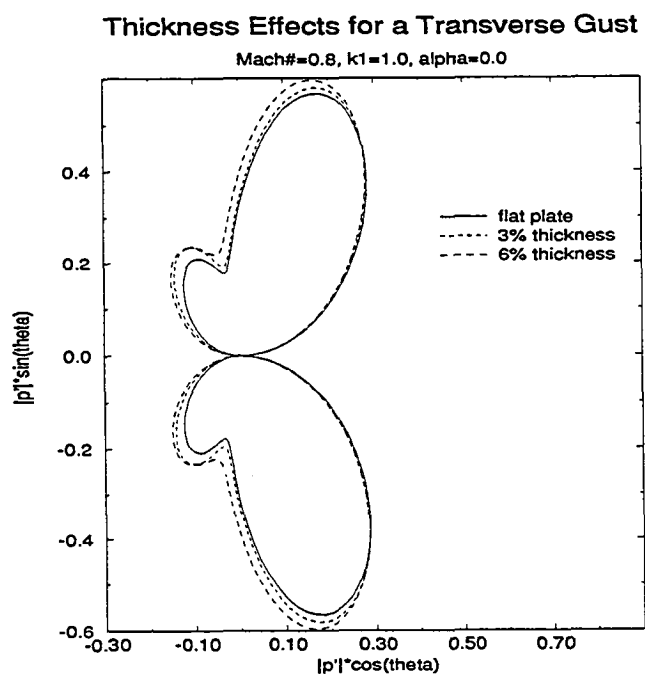


Figure 13.

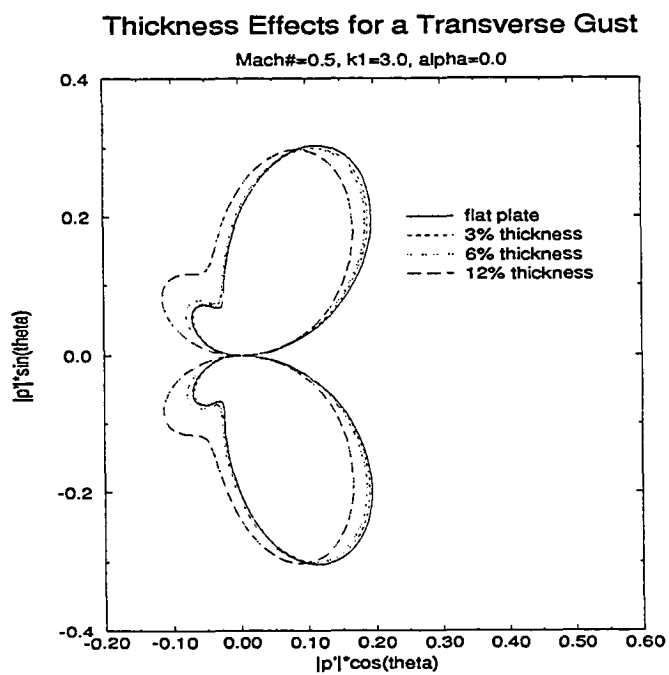


Figure 14.

Kirchoff Radius Effect for Airfoil in a Transverse Gust

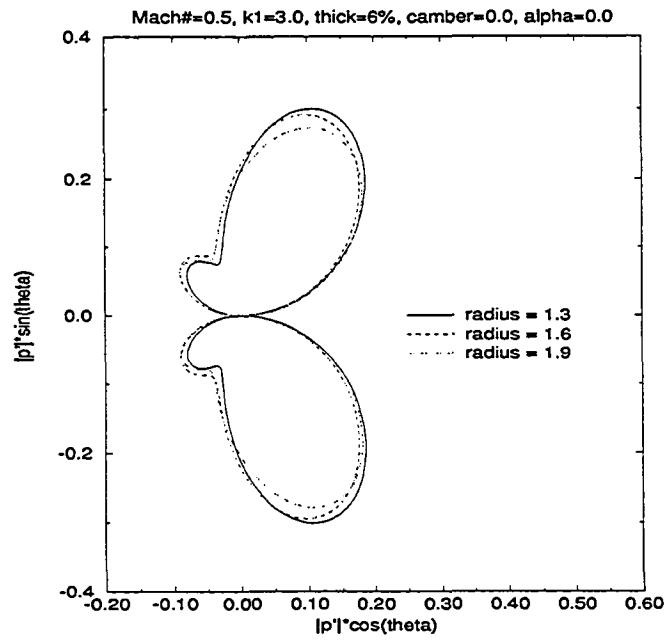


Figure 15.

Angle of Attack Effects for a Transverse Gust

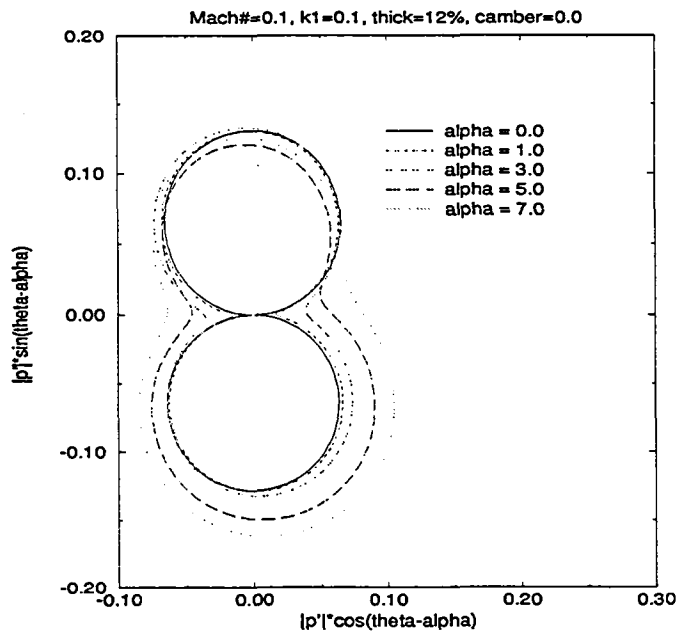


Figure 16.

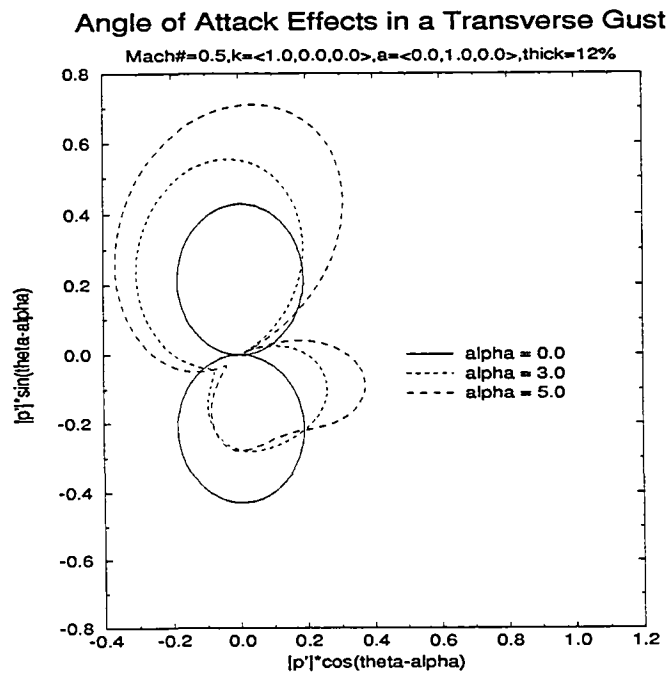


Figure 17.

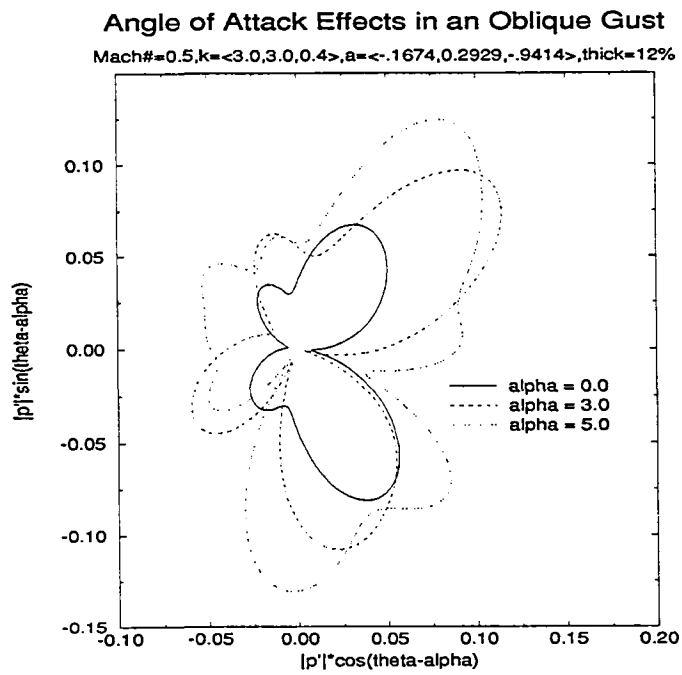


Figure 18.

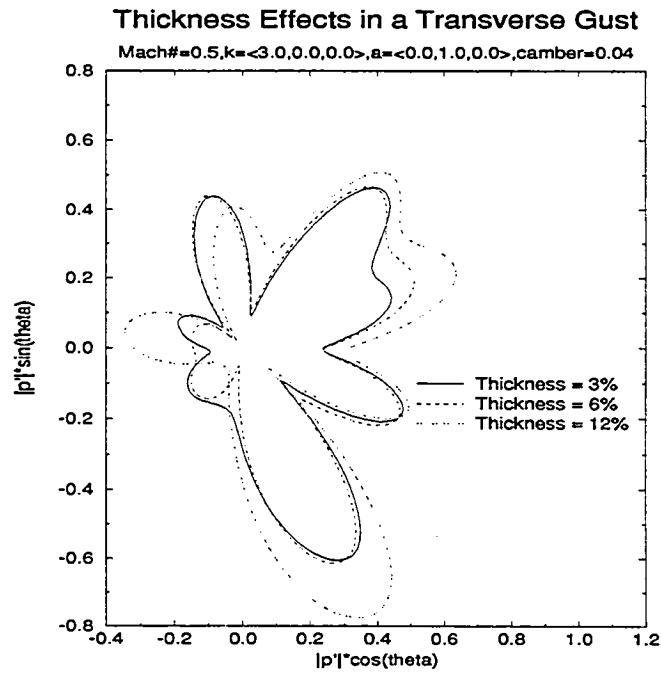


Figure 19.

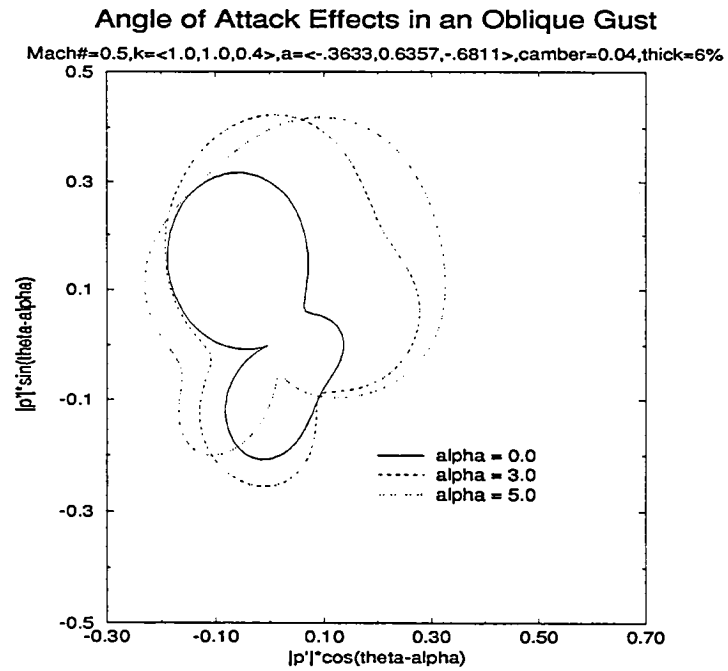


Figure 20.

REPORT DOCUMENTATION PAGE			Form Approved OMB No. 0704-0188	
Public reporting burden for this collection of information is estimated to average 1 hour per response, including the time for reviewing instructions, searching existing data sources, gathering and maintaining the data needed, and completing and reviewing the collection of information. Send comments regarding this burden estimate or any other aspect of this collection of information, including suggestions for reducing this burden, to Washington Headquarters Services, Directorate for Information Operations and Reports, 1215 Jefferson Davis Highway, Suite 1204, Arlington, VA 22202-4302, and to the Office of Management and Budget, Paperwork Reduction Project (0704-0188), Washington, DC 20503.				
1. AGENCY USE ONLY (Leave blank)	2. REPORT DATE December 1995	3. REPORT TYPE AND DATES COVERED Technical Memorandum		
4. TITLE AND SUBTITLE Potential Theoretic Methods for Far Field Sound Radiation Calculations		5. FUNDING NUMBERS WU-505-90-5K		
6. AUTHOR(S) S.I. Hariharan, Edward J. Stenger, and J.R. Scott				
7. PERFORMING ORGANIZATION NAME(S) AND ADDRESS(ES) National Aeronautics and Space Administration Lewis Research Center Cleveland, Ohio 44135-3191		8. PERFORMING ORGANIZATION REPORT NUMBER E-10028		
9. SPONSORING/MONITORING AGENCY NAME(S) AND ADDRESS(ES) National Aeronautics and Space Administration Washington, D.C. 20546-0001		10. SPONSORING/MONITORING AGENCY REPORT NUMBER NASA TM-107118 ICOMP-95-25		
11. SUPPLEMENTARY NOTES S.I. Hariharan, Institute for Computational Mechanics in Propulsion, NASA Lewis Research Center (work funded under NASA Cooperative Agreement NCC3-370) and The University of Akron, Akron, Ohio 44325; Edward J. Stenger, The University of Akron, Akron, Ohio 44325; J.R. Scott, NASA Lewis Research Center. ICOMP Program Director, Louis A. Povinelli, organization code 2600, (216) 433-5818.				
12a. DISTRIBUTION/AVAILABILITY STATEMENT Unclassified - Unlimited Subject Categories 64 and 71 This publication is available from the NASA Center for Aerospace Information, (301) 621-0390.			12b. DISTRIBUTION CODE	
13. ABSTRACT (Maximum 200 words) In the area of computational acoustics, procedures which accurately predict the far-field sound radiation are much sought after. A systematic development of such procedures are found in a sequence of papers by Atassi. The method presented here is an alternate approach to predicting far field sound based on simple layer potential theoretic methods. The main advantages of this method are: it requires only a simple free space Green's function, it can accommodate arbitrary shapes of Kirchoff surfaces, and is readily extendable to three-dimensional problems. Moreover, the procedure presented here, though tested for unsteady lifting airfoil problems, can easily be adapted to other areas of interest, such as jet noise radiation problems. Results are presented for lifting airfoil problems and comparisons are made with the results reported by Atassi. Direct comparisons are also made for the flat plate case.				
14. SUBJECT TERMS Compressible flows; Aeroacoustics; Singular integral equations			15. NUMBER OF PAGES 32	
			16. PRICE CODE A03	
17. SECURITY CLASSIFICATION OF REPORT Unclassified	18. SECURITY CLASSIFICATION OF THIS PAGE Unclassified	19. SECURITY CLASSIFICATION OF ABSTRACT Unclassified	20. LIMITATION OF ABSTRACT	

National Aeronautics and
Space Administration

Lewis Research Center

Cleveland, OH 44135-3191

ICOMP OAI

Official Business

Penalty for Private Use \$300

